

GROWTH AND CHARACTERIZATION OF SOLUTION GROWN NONLINEAR OPTICAL AMMONIUM TARTRATE CRYSTAL

N. Kalaimani¹, K. Ramya², R. Aarthi³ and C. Ramachandra Raja^{3,*}

¹Department of Physics, Thiru.Vi.Ka Government Arts College,
Thiruvarur-610 003, Tamilnadu, India.

²Department of Physics, TUK Arts College, Thanjavur-613 002, Tamilnadu, India.

³Department of Physics, Government Arts College (Autonomous),
Kumbakonam-612 002, Tamilnadu, India.

*E-mail: crrajaphy@gmail.com

ABSTRACT

Ammonium tartrate single crystals were grown by a solvent evaporation method. The single crystal and powder X-ray diffraction studies determine the lattice parameter and showed that the crystal is monoclinic. The lower cut off wavelength was found at 220nm. The functional groups such as OH, NH₄⁺, COO⁻, and CH declares the formation of ammonium tartrate crystal. The molecular structure was established from the NMR analysis. The thermal studies were carried out from TG/DTA experiments. The second harmonic generation efficiency was measured through Kurtz-Perry technique. The observed second harmonic generation efficiency was found to be higher than KDP and some of the reported nonlinear optical crystals.

Keywords: Ammonium tartrate, XRD analysis, FTIR analysis, NMR analysis, Second harmonic generation efficiency.

© RASAYAN. All rights reserved

INTRODUCTION

Nonlinear optical crystals, in recent years, were studied widely due to their wide application in various technologies like optical information processing, data storage and computing¹⁻⁵. They are useful in various fields as a result of its high second-order optical nonlinearity, wide transmission range, good thermal and mechanical stability. In semi-organic crystals, the organic molecule binds and form a stable complex with an inorganic host which results in the development of new crystal having high optical nonlinearity⁶. The proper combination of organic and inorganic compound results in a good quality semi-organic crystal and they can play a better role in various linear and nonlinear applications⁷. The crystal derivatives of ammonium are used as optical modulators and frequency converters⁸. The tartaric acid is a α -hydroxyl carboxylic acid which when reacts with various salts produces a material that is suitable for second harmonic generation process. This article reports the growth of ammonium tartrate crystal from solution growth method. The structural characterization of ammonium tartrate crystal was reported by Yadav et al.⁹, the characterization of ammonium tartrate crystal was done here.

MATERIALS AND METHODS

Ammonium tartrate crystal was obtained by solution grown solvent evaporation method. Ammonium carbonate and tartaric acid were taken in an equimolar ratio (1:1) and the solvent used here was double distilled water. The mixture was stirred well using a magnetic stirrer and a homogeneous saturated solution was obtained after 3 hours. This saturated solution was filtered using Whatmann filter paper. Then the filtered solution was covered using polythene paper and a few holes were made for solvent evaporation.

After 30 days colorless crystals were harvested. Figure-1 shows the photograph of grown ammonium tartrate crystals. The reaction scheme and the molecular structure of the grown crystal is given below.

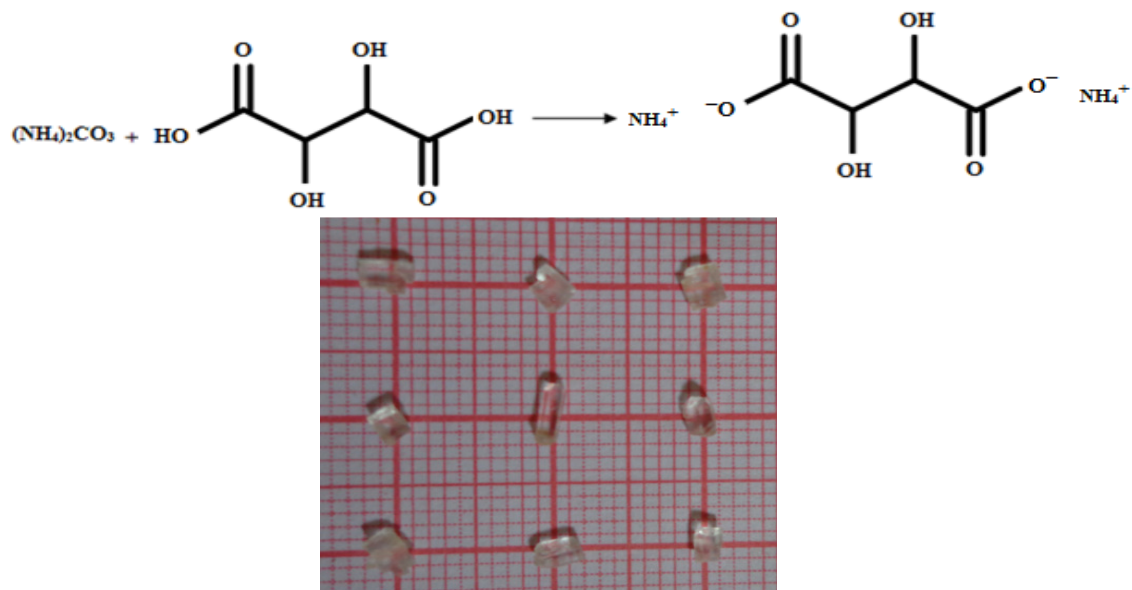


Fig.-1: Photograph of Ammonium Tartrate Crystal

RESULTS AND DISCUSSION

Single Crystal and Powder X-Ray Diffraction Analysis

Transparent crystals of ammonium tartrate were subjected to single and powder crystal X-ray diffraction studies. Single crystal XRD studies were carried out using NONIUS CAD4 single crystal X-ray diffractometer with $\text{MoK}\alpha$ ($\lambda = 0.71069 \text{ \AA}$) radiation and reveal that the crystal system is monoclinic with P2_1 space group.

Powder X-ray diffraction analysis was done using Rich Seifert diffractometer with $\text{CuK}\alpha$ ($\lambda = 1.54060 \text{ \AA}$) radiation and is shown in Fig.-2. From the XRD pattern, the lattice parameters were calculated using unit cell software, and the parameter is found to be same as that obtained from single crystal XRD. The comparison of lattice parameter obtained from single crystal and powder XRD with reported values⁹ are given in Table-1.

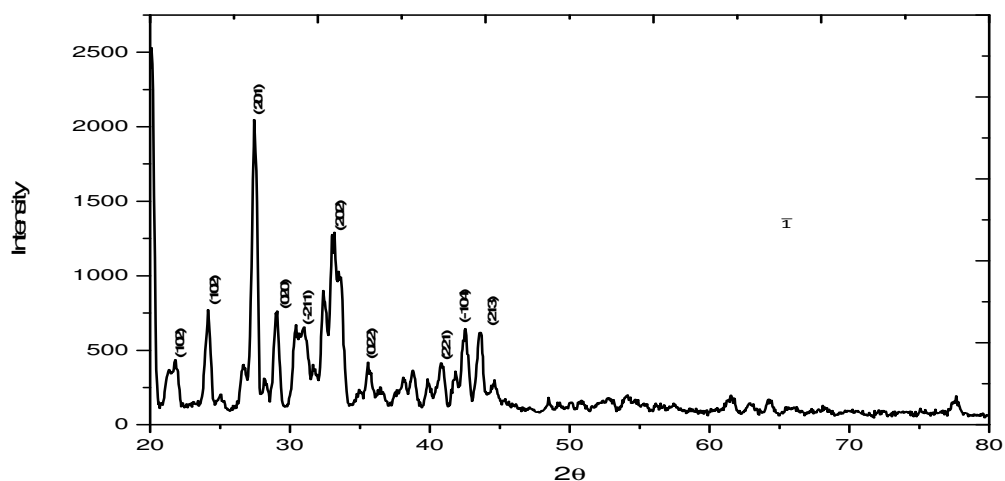


Fig.-2: Powder XRD Pattern of Ammonium Tartrate Crystal

Table-1: Lattice Parameter of Ammonium Tartrate Crystal

Lattice Parameters	Ammonium Tartrate Crystal		Reported Values [9]
	Single Crystal XRD	Powder XRD	
a(Å)	7.042(2)	7.0961	7.083(1)
b(Å)	6.101(1)	6.1148	6.128(3)
c(Å)	8.762(5)	8.8808	8.808(1)
α (°)	90	90	90
β (°)	92.36	92.98	92.42
γ (°)	90	90	90

Optical Transmission Spectral Study

The optical transparency range was observed from Perkin-Elmer UV-Vis-NIR spectrometer in the range 190 to 1100 nm. The transmission spectrum of the grown crystal is shown in Fig.-3. From the figure, it is observed that the grown crystal has the good transmission in the entire visible region and up to 220 nm in the UV region. The lower cut off wavelength occurs around 220nm and the band gap is found to be 5.045 eV. Any nonlinear optical material can be used only in the absence of absorption at fundamental and harmonic wavelengths. Hence this crystal can be used to generate wavelengths up to 220 nm and in optoelectronic applications^{10,11}.

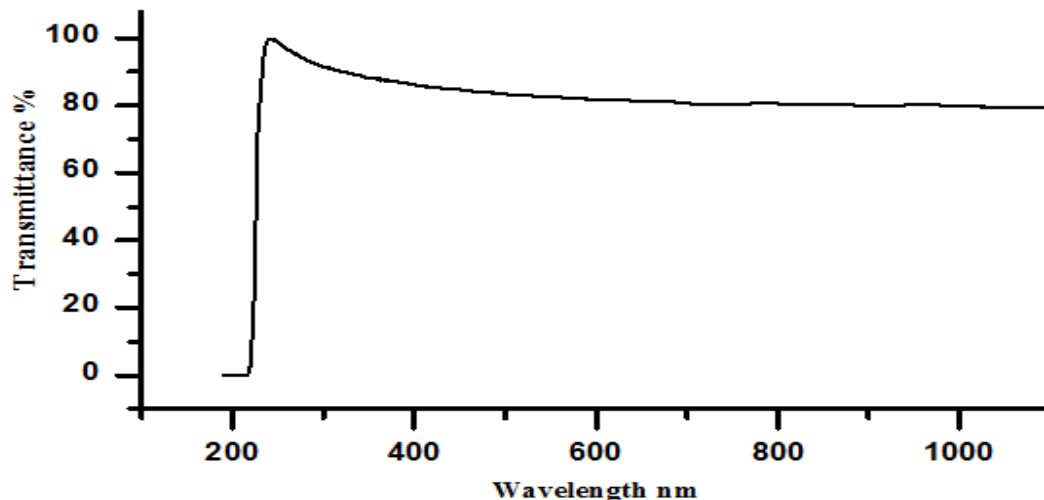


Fig.-3: UV-Vis-NIR Spectrum of Ammonium Tartrate Crystal

FT IR and FT Raman Spectral Analyses

Fourier Transform infrared spectrum was recorded by the KBr pellet technique using a SPECTROMRXI FTIR spectrometer and FT Raman spectrum was recorded using a BRUKER RFS 27 spectrometer to confirm the functional groups. The FTIR and FT Raman spectra of ammonium tartrate crystal are given in Fig.-4 and 5 respectively. The broadening of peaks in the higher wavenumber region between 2800 cm^{-1} and 3400 cm^{-1} in IR and Raman are assigned to the vibrations of OH, NH_4^+ and CH stretching vibrations. The NH_4^+ asymmetric stretching was observed in IR at 3215 cm^{-1} and 3243 in Raman spectra. This increase in wavenumber of NH_4^+ asymmetric stretching confirms the formation of hydrogen bond N-H...O in the ammonium tartrate crystal¹². The stretching vibration of the C-H bond of tartrate anion was observed at 2925 cm^{-1} in IR and 2968 cm^{-1} in Raman spectra respectively.

The peak at 1707 cm^{-1} in IR and 1704 cm^{-1} in Raman are attributed to C=O stretching vibration. The band present at 1556 cm^{-1} and 1401 cm^{-1} in IR and 1535 cm^{-1} and 1395 cm^{-1} in Raman are due to the asymmetric and symmetric stretching vibration of COO^- group. Here the decrease in wavenumber of carbonyl stretching groups was due to the presence of hydrogen bond in the crystal¹². The rocking vibration of NH_4^+ group was observed at 1072 cm^{-1} and 1071 cm^{-1} in IR and Raman respectively. The C-H out of plane bending vibration occurs at 901 cm^{-1} and 902 cm^{-1} in IR and Raman respectively. The vibrational frequencies and their corresponding assignments are given in Table-2.

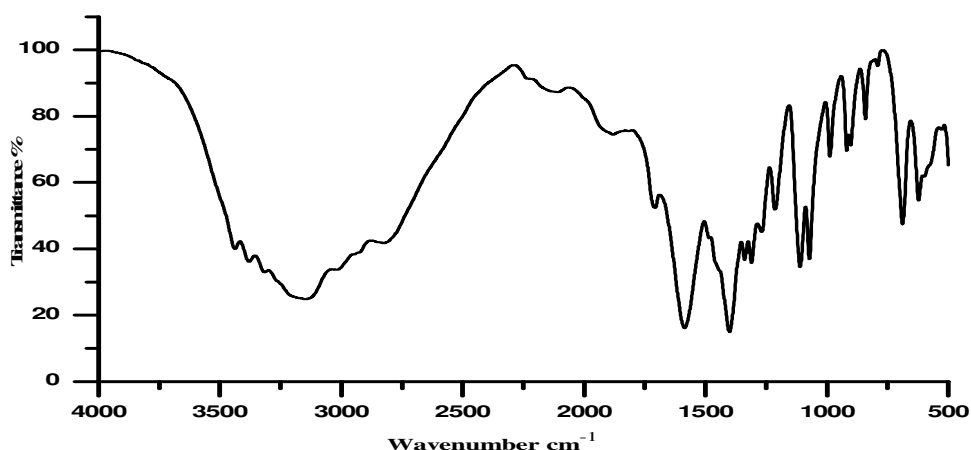


Fig.-4: FTIR Spectrum of Ammonium Tartrate Crystal

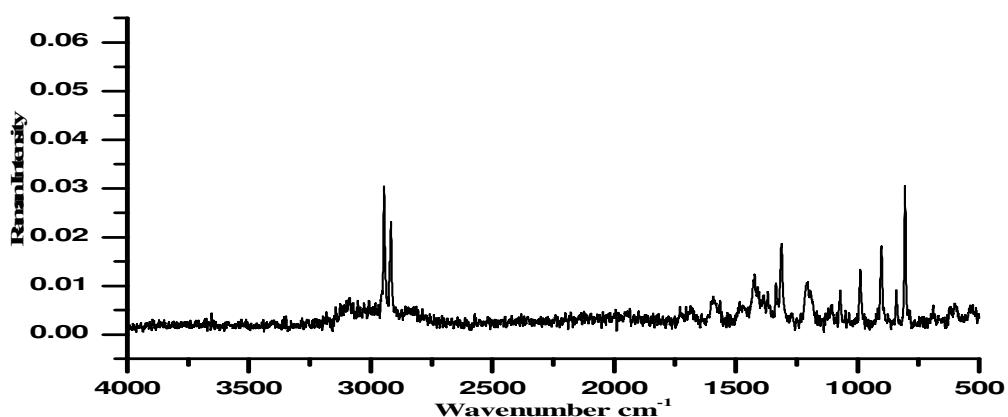


Fig.-5: FT Raman Spectrum of Ammonium Tartrate Crystal

Table-2: Observed Vibrational Wavenumbers and Their Assignments

Wavenumber cm ⁻¹		Assignments
FTIR	FT Raman	
3315	-	OH stretching
3215	3243	NH ₄ ⁺ asymmetric stretching
3097	3086	NH ₄ ⁺ symmetric stretching
2925	2968	C-H stretching
1707	1704	C=O stretching
1556	1535	COO ⁻ asymmetric stretching
1401	1395	COO ⁻ symmetric stretching
1268	1204	C-H in-plane bending
1072	1071	NH ₄ ⁺ rocking
901	902	C-H out of plane bending
688	688	O-H out of plane bending

¹H and ¹³C NMR Spectral Analysis

The NMR technique was used to detect the presence of proton and carbon in the grown crystal. The ¹H NMR and ¹³C NMR spectra were recorded at room temperature with D₂O as solvent using Bruker instrument (operated at 300MHz for ¹H NMR and 75MHz for ¹³C NMR). Figure-6 shows the ¹H NMR spectrum of ammonium tartrate crystal. The chemical shift values for ¹H NMR and ¹³C NMR spectra are

given in Table-3. The peak observed at $\delta = 4.703\text{ppm}$ was due to the solvent D_2O . The resonance peak at $\delta = 2.378\text{ppm}$ was due to the OH group and the peak appeared at $\delta = 4.213\text{ppm}$ was due to the CH proton of tartaric acid. The CH proton of parent tartaric acid produces a shift at $\delta = 4.34\text{ppm}$. Thus, the upfield shift of CH proton in ammonium tartrate crystal confirms the formation of the crystal. Then the signal produced at $\delta = 3.97\text{ppm}$ corresponds to the NH_4^+ proton of ammonium tartrate crystal¹³. The disappearance of the signal for the acid proton in NMR of the diammonium tartrate crystal indicates that the acid proton ($-\text{COOH}$) of the tartaric acid involved in bond formation with the ammonium forming diammonium tartrate crystal.

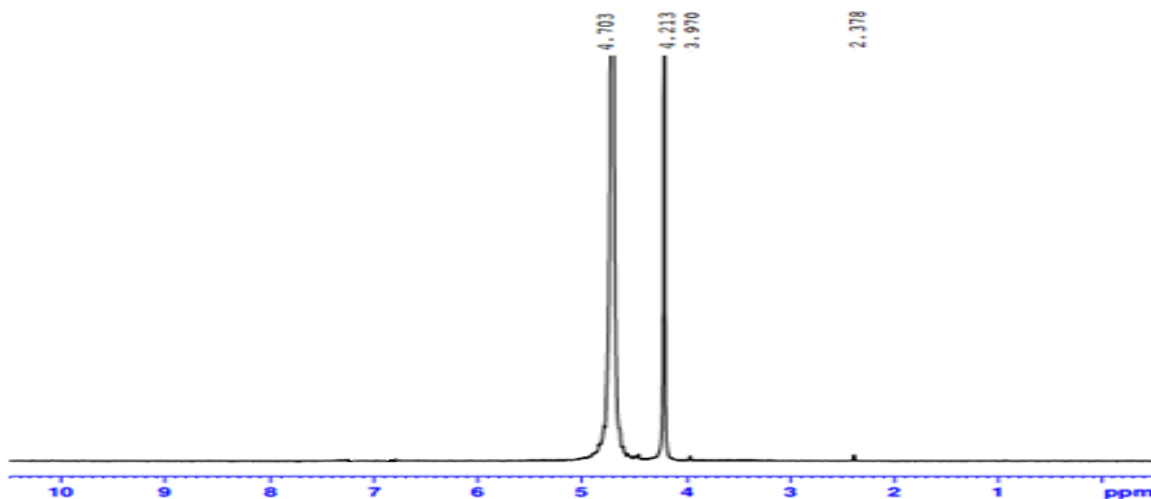


Fig.-6: ^1H NMR of Ammonium Tartrate Crystal

Table-3: Chemical Shifts in ^1H and ^{13}C NMR Spectra of Ammonium Tartrate Crystal

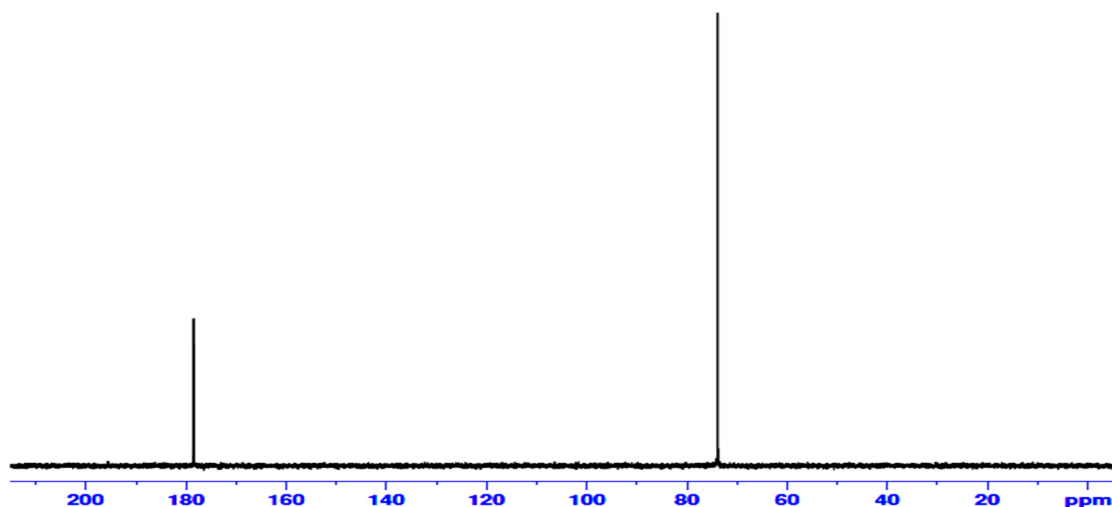
Spectra	Chemical Shift	Group Identification
^1H NMR	2.378	OH
	3.97	NH_4^+
	4.213	CH
	4.703	D_2O solvent
^{13}C NMR	178.4	$-\text{COOH}$
	73.81	$-\text{CH}=\text{}$

The ^{13}C NMR spectrum of ammonium tartrate crystal is shown in Fig.-7. The resonance peak at $\delta = 178.4\text{ppm}$ was due to the presence of COOH group of ammonium tartrate crystal. The peak value of the COOH group of pure tartaric acid was observed at $\delta = 175.25\text{ppm}$ ¹⁴. Thus the peak was shifted towards downfield, and the downfield shift was due to the formation of a bond between ammonium and tartaric acid, which confirms the formation of ammonium tartrate crystal. The peak appearing at $\delta = 73.81\text{ppm}$ corresponds to the downfield of CH carbon of tartaric acid.

Differential thermal analysis (DTA) and thermogravimetric analysis (TGA) were carried out in the temperature range $30\text{-}500^\circ\text{C}$ using an instrument NETZSCH SDT Q600 V 8.3 build 101 in a nitrogen atmosphere at a heating rate of $20^\circ\text{C}/\text{min}$. The TG/DTA curve of ammonium tartrate crystal is given in Figure 8. In the TG curve, there is a weight loss of nearly 75% around 252°C . This is in accordance with the endothermic peak observed at 252.15°C in DTA and this may correspond to the simultaneous melting and decomposition of the crystal. The next weight loss of nearly 25% observed between 252°C to 500°C indicates the complete decomposition of the crystal.

Nonlinear Optical Study

The second harmonic generation efficiency of the crystal was ascertained from Kurtz and Perry powder technique¹⁵. The powdered sample of the crystal was subjected to Q-switched mode-locked Nd:YAG laser with $1.4\text{mJ}/\text{pulse}$ of input energy.

Fig.-7: ^{13}C NMR of Ammonium Tartrate Crystal

The green light emitted from the sample establishes the frequency conversion property of the crystal. A second harmonic signal of 88mV for ammonium tartrate crystal and 55mV for the reference KDP were observed. Thus, the second harmonic generation efficiency of ammonium tartrate crystal was 1.6 times greater than that of KDP. The output of the second harmonic generation is based on the molecular structure and the charge transfer between the bonding groups^{16,17}. N-H...O hydrogen bond results in higher second harmonic generation efficiency of the ammonium tartrate crystal. The second harmonic generation efficiency is compared with some other nonlinear optical crystals and is given in Table-4. The compared second harmonic generation efficiency shows that the grown ammonium tartrate crystal has good SHG efficiency.

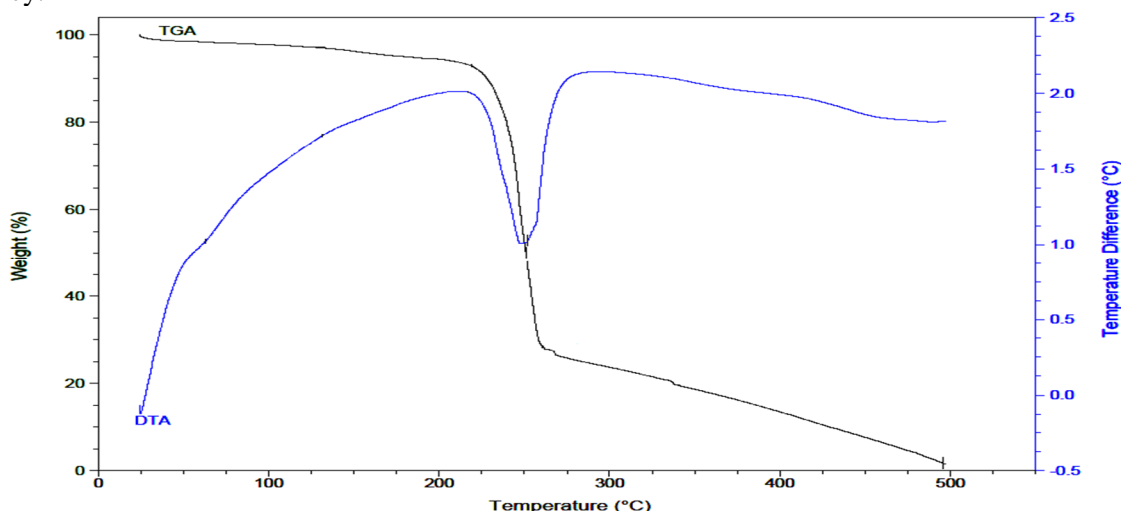


Fig.-8: TG/DTA Curve of Ammonium Tartrate Crystal

Table-4: Second Harmonic Generation Efficiency of Ammonium Tartrate Crystal with Some Nonlinear Optical Crystals

Crystal Name	Relative SHG Efficiency (KDP)	Reference
Ammonium Tartrate	1.6	Present work
Ammonium hydrogen L-tartrate	1.02	[13]
Ammonium D, L-Tartrate	1.3	[17]
L-histidinium-L-tartrate hemihydrate	0.79	[18]
L-lysine-L-tartaric acid	0.35	[19]

CONCLUSION

Ammonium tartrate crystals have been grown from an aqueous solution by a solvent evaporation method. The single and powder x-ray diffraction analyses determine the lattice parameter and confirm that the crystal is monoclinic. The lower cut off wavelength was observed at 220nm. The functional groups were identified from IR and Raman spectral analyses. The ^1H and ^{13}C NMR reveals the molecular structure of the grown crystal. The thermal stability of the grown crystal was studied. The second harmonic generation efficiency of Ammonium tartrate crystal was 1.6 times greater than that of KDP.

ACKNOWLEDGMENT

The authors thank the sophisticated analytical instruments facility (SAIF), Indian Institute of Technology (IITM), Chennai for providing single crystal XRD and FT Raman spectrum and gratefully acknowledge the Instrumentation center of St. Joseph's College, Trichy for recording FTIR and UV-Vis-NIR spectra. The authors wish to thank CECRI, Karaikudi, for powder XRD and TG/DTA studies and SASTRA University, Thanjavur for NMR studies. The authors are also grateful to Dr. P. K. Das, Indian Institute of Science, Bangalore for the measurement of SHG efficiency.

REFERENCES

1. Manoj K. Gupta, Nidhi Sinha, Binay Kumar, *Physica B. Condensed Matter Physics*, **406**, 63(2011), DOI:10.1016/j.physb.2010.10.016
2. P. V. Dhanaraj, N. P. Rajesh, G. Vinitha, G. Bhagavannarayana, *Materials Research Bulletin*, **46**, 726 (2011), DOI: 10.1016/j.materresbull.2011.01.013
3. M. Lydia Caroline, R. Sankar, R. M. Indirani, S. Vasudevan, *Materials Chemistry and Physics*, **114**, 490 (2009), DOI:10.1016/j.matchemphys.2008.09.070
4. A. Bhaskaran, C. M. Raghavan, R. Mohankumar, R. Jayavel, *Current Applied Physics*, **10**, 1261 (2010), DOI:10.1016/j.cap.2010.03.004
5. N. Vijayan, S. Rajasekaran, G. Bhagavannarayana, R. Ramesh Babu, R. Gopalakrishnan, M. Palanichamy, P. Ramasamy, *Crystal Growth Design*, **6**, 2441 (2006), DOI:10.1021/cg049594y
6. S. Moitra, T. Kar, Crystal, *Research Technology*, **45**, 70(2010), DOI: 10.1002/crat.200900447
7. R. Subhashini, S. Arjunan, *Optics and Laser Technology*, **101**, 248(2018), DOI:10.1016/j.optlastec.2017.11.009
8. X. Ren, D. Xu, D. Xue, *Journal of Crystal Growth*, **310**, 2005(2008), DOI:10.1016/j.jcrysgro.2007.11.008
9. V. S. Yadava, V. M. Padmanabhan, *Acta Crystallographica*, **B29**, 493(1973), DOI:10.1107/S0567740873002803
10. G. Anandha babu, G. Bhagavannarayana, P. Ramasamy, *Journal of Crystal. Growth*, **310**, 1228 (2008), DOI:10.1016/j.jcrysgro.2007.12.024
11. M. Toulemonde, C. Dufour, E. Parrmier, *Physics Review*, **B46**, 14362(1992), DOI:10.1103/PhysRevB.46.14362
12. S. Vidya, C. Ravikumar, I. Hubert Joe, P. Kumaradhas, B. Devipriya, K. Raju, *Journal of Raman Spectroscopy*, **42**, 676(2011), DOI:10.1002/jrs.2743
13. Redrothu Hanumantharao, S. Kalainathan, G. Bhagavannarayana, U.Madhusoodanan, *Spectrochimica. Acta Part A*, **103**, 388 (2013), DOI:10.1016/j.saa.2012.10.044
14. S. K. Kurtz, T. T. Perry, *Journal of Applied Physics*, **39**, 3813 (1968), DOI: 10.1063/1.1656857
15. T. Uma Devi, N. Lawrence, R. Ramesh Babu, K. Ramamurthi, *Journal of Crystal Growth*, **310**, 116(2008), DOI:10.1016/j.jcrysgro.2007.10.011
16. S. A. Martin Britto Dhas, G. Bhagavannarayana, S. Natarajan, *Journal of Crystal Growth*, **310**, 3535(2008), DOI:10.1016/j.jcrysgro.2008.04.049
17. D. Joseph Daniel, P. Ramasamy, *Materials Research Bulletin*, **47**, 708(2012), DOI:10.1016/j.materresbull.2011.12.009
18. M. K. Marchewka, S. Debrus, A. Pietraszko, A. J. Barnes, H. Ratajczak, *Journal of Molecular Structure*, **656**, 265 (2003), DOI:10.1016/s0022-2860(03)00352-1
19. S. Debrus, M. K. Marchewka, J. Baran, M. Drozd, R. Czopnik, A. Pietraszko, H. Ratajczak, *Journal of Solid State Chemistry*, **178**, 2880 (2005), DOI:10.1016/j.jssc.2005.06.029

[RJC-4019/2018]